タイトル Title	Influence of the structure of the anion in an ionic liquid electrolyte on the electrochemical performance of a silicon negative electrode for a lithium-ion battery
著者 Auther(s)	Yamaguchi, Kazuki; Domi, Yasuhiro; Usui, Hiroyuki; Shimizu, Masahiro; Matsumoto, Kuninobu; Nokami, Toshiki; Itoh, Toshiyuki; Sakaguchi, Hiroki
掲載誌・巻号・ページ Citation	Journal of Power Sources , 338 : 103 - 107
刊行日 Issue Date	2017-01-15
資源タイプ Resource Type	学術雑誌論文 / Journal Article
版区分 Resource Version	著者版 / Author
権利 Rights	Copyright © 2017 Elsevier B.V. All rights reserved. This manuscript version is made available under the CC-BY-NC-ND 4.0 license https://creativecommons.org/licenses/by-nc-nd/4.0/
DOI	10.1016/j.jpowsour.2016.10.111
URL	http://repository.lib.tottori-u.ac.jp/5488

Influence of the Structure of the Anion in an Ionic Liquid Electrolyte on the Electrochemical Performance of a Silicon Negative Electrode for a Lithium-Ion Battery

Kazuki Yamaguchi[a,b], *Yasuhiro Domi*[a,b], *Hiroyuki Usui*[a,b], *Masahiro Shimizu*[a,b], *Kuninobu Matsumoto*[a,b], *Toshiki Nokami*[a,b], *Toshiyuki Itoh*[a,b], *and Hiroki Sakaguchi*[a,b,*]

[a]Department of Chemistry and Biotechnology, Graduate School of Engineering, Tottori University

4-101 Minami, Koyama-cho, Tottori 680-8552, Japan

[b]Center for Research on Green Sustainable Chemistry, Tottori University

4-101 Minami, Koyama-cho, Tottori 680-8552, Japan

*Corresponding author Tel./Fax: +81-857-31-5265, e-mail: sakaguch@chem.tottori-u.ac.jp

Keywords: Silicon; Li-ion battery; Ionic liquid electrolyte; Anion; Gas-deposition

Abstract

We investigated the influence of the anions in ionic liquid electrolytes on the electrochemical performance of a silicon (Si) negative electrode for a lithium-ion battery. While the electrode exhibited poor cycle stability in tetrafluoroborate-based and propylene carbonate-based electrolytes, better cycle performance was achieved in bis(fluorosulfonyl)amide (FSA^-)- and bis(trifluoromethanesulfonyl)amide ($TFSA^-$)-based electrolytes, in which the discharge capacity of a Si electrode was more than 1000 mA h g^{-1} at the 100th cycle. It is considered that a surface film derived from FSA^-- and $TFSA^-$-based electrolytes effectively suppressed continuous decomposition of the electrolyte. In a capacity limitation test, a discharge capacity of 1000 mA h g^{-1} was maintained even after about the 1600th cycle in the FSA^--based electrolyte, which corresponds to a cycle life almost twice as long as that in $TFSA^-$-based electrolyte. This result should be explained by the high structural stability of FSA^--derived surface film. In addition, better rate capability with a discharge capacity of 700 mA h g^{-1} was obtained at a high current rate of 6 *C* (21 A g^{-1}) in FSA^--based electrolyte, which was 7-fold higher than that in $TFSA^-$-based electrolyte. These results clarified that FSA^--based ionic liquid electrolyte is the most promising candidate for Si-based negative electrodes.

1. Introduction

Lithium-ion batteries (LIBs) have been widely used in portable devices such as smartphones and laptops due to their high energy density. Although an additional increase in energy density is needed before LIBs can be used as a power source in electric vehicles and stationary supply systems, the capacity of a graphite negative electrode, which is used currently, is insufficient. Since Lai reported solid lithium–silicon electrode could operate at 400 ºC [1], silicon (Si) is a promising active material as a negative electrode material for next-generation LIBs because it has a remarkably high theoretical capacity of 3580 mA h g^{-1} ($Li_{15}Si_4$) [2,3]. However, Si undergoes a huge change in volume during alloying/dealloying reactions with Li [4,5], and this generates high stress and strain in the active material. The accumulation of strain during repeated charge-discharge cycling brings about disintegration of the active material layer, which results in poor cyclability for a Si electrode. To overcome this issue, a nano-sized silicon has been studied as one of the promising approaches. Wu et al. demonstrated that nano-sized Si-coated graphite retained a relatively high reversible capacity of 567 mA h g^{-1} over 20 cycles [6]. It was reported that vacuum deposited Si films on rough Ni and Cu substrates exhibited excellent cyclability, and the film consisted of nano-particles with polycrystalline kept structure stable against volumetric change during Li-insertion/extraction [7].

The electrolyte is one of the most important components that determines battery performance and safety. A non-flammable electrolyte is needed for next-generation LIBs with a high energy density to enhance their safety since the risk of ignition should increase with the energy density.

Thus, we have focused on identifying an ionic liquid with excellent physicochemical properties, such as incombustibility, negligible vapor pressure, and a wide electrochemical window. We previously reported that the cycling stability of a Si-alone electrode in a certain ionic liquid electrolyte was superior to that in a conventional organic electrolyte [8–10]. However, the initial reversible capacity in the former electrolyte is lower than that in the latter electrolyte because Li^+ exhibits very strong electrostatic interaction with the anion of the ionic liquid, and thus Li^+ undergoes very slow desolvation from the anion. To overcome this problem, we introduced an ether group, i.e., a 2-methoxyethoxymethyl group, into the side chain of the cation of the ionic liquid, and revealed that this significantly increased the initial capacity of a Si electrode [11]. It is considered that the partial negative charge of the oxygen atom in the ether group weakens the electrostatic interaction between Li^+ and the anion of the ionic liquid and promotes the desolvation of Li^+, which leads to smooth Li^+ transport at the interface between the electrode and the electrolyte. These results suggest that the structure of the cation in the ionic liquid electrolyte strongly influences the electrochemical performance of a Si negative electrode.

The anion of an ionic liquid electrolyte is also an important factor because it should affect the solvation structure of Li^+, ionic conductivity, viscosity and so on [12–14]. For example, the solvation structure of Li^+ in a bis(fluorosulfonyl)amide (FSA^-)-based ionic liquid electrolyte is different from that in a bis(trifluoromethanesulfonyl)amide ($TFSA^-$)-based electrolyte, even though FSA^- and $TFSA^-$ are based on the same amide. Li^+ forms $[Li(TFSA)_2]^-$ and $[Li(FSA)_3]^{2-}$ ion clusters in

$TFSA^-$- and FSA^--based ionic liquid electrolytes, respectively [15–17]. While the relationship between the structure of the anion in an ionic liquid electrolyte and the electrochemical performance of a negative electrode other than a Si-based electrode (e.g., graphite) has been reported [18–20], there have been no systematic studies for Si-based electrodes. In this study, we investigated the effect of the structure of the anion in an ionic liquid electrolyte on the electrochemical performance of a Si negative electrode for use in a LIB. Notably, we used ionic liquid electrolytes with a single anion species; i.e. the anion of the Li salt was the same as that of the ionic liquid.

2. Experimental

Si powder (Wako Pure Chemical Industries, Ltd., 99.9%) was used as an active material. A Si electrode was prepared by the gas-deposition method without any conducting additive or binder. The detailed conditions have been described in our previous papers [10,11]. The weight of the deposited active materials and the deposition area on the Cu substrate were ca. 30 μg and 0.80 cm^2, respectively. We assembled a 2032-type coin cell consisting of the Si electrode as a working electrode, Li metal foil (Rare Metallic Co., Ltd., 99.90%) as a counter electrode, and a glass fiber filter (Whatman GF/A) as a separator. The ionic liquid used in this study consisted of 1-((2-methoxyethoxy)methyl)-1-methylpiperidinium ($PP1MEM^+$) cation and three types of anion, i.e., FSA^-, $TFSA^-$, or tetrafluoroborate (BF_4^-), as shown in Figure S1. The electrolyte solution used was 1 mol dm^{-3} Li*X*-dissolved in PP1MEM-*X* (*X*: FSA, TFSA, or BF_4). 1 mol dm^{-3} LiTFSA in

propylene carbonate (PC; $C_4H_6O_3$, Kishida Chemical Co., Ltd.) was also used as a conventional organic electrolyte. The preparation of electrolyte solution and cell assembly were performed in an Ar-filled glove box (Miwa MFG, DBO-2.5LNKP-TS) with a dew point below −100 °C and oxygen content below 1 ppm. A galvanostatic charge-discharge test was conducted using an electrochemical measurement system (HJ-1001SD8, Hokuto Denko Co., Ltd.) in a potential range between 0.005 and 2.000 V vs. Li^+/Li at 303 K under a current density of 0.42 A g^{-1} (0.12 *C*). The high-rate performance of the electrodes was investigated at a current rate from 0.12 *C* to 12 *C*. The ionic conductivity of ionic liquid electrolytes was also investigated by an electrochemical impedance spectroscopic analysis in the frequency range from 100 kHz to 500 Hz with a potential amplitude of 10 mV.

3. Results and discussion

Figure 1(a) shows the dependence of the discharge (Li-extraction) capacity of a Si-alone negative electrode on the cycle number in various ionic liquid electrolyte solutions. For comparison, the result in an organic electrolyte (1 mol dm^{-3} LiTFSA/PC) is also shown. While the discharge capacity of a Si electrode was as high as 3000 mA h g^{-1} in the first cycle in the PC-based electrolyte solution, it rapidly decayed; the Si electrode showed poor cycling stability in the PC-based electrolyte. The rapid capacity-fading resulted from disintegration of the active material layer due to the large change in the volume of Si during Li-insertion and extraction [5]. The volumetric change brought about the cracking and pulverization of Si, and followed by electrolyte decomposition on the

exposed surface of the electrode. This phenomenon led to a drop in Coulombic efficiency at around the 30th cycle in the PC-based electrolyte, as shown in Figure 1(b). The initial discharge capacity of a Si electrode was less than 800 mA h g^{-1} in the BF_4^--based electrolyte solution. The cycle performance of the electrode in the BF_4^--based electrolyte was almost the same as that in the PC-based electrolyte; the discharge capacity was less than 200 mA h g^{-1} at the 80th cycle in both

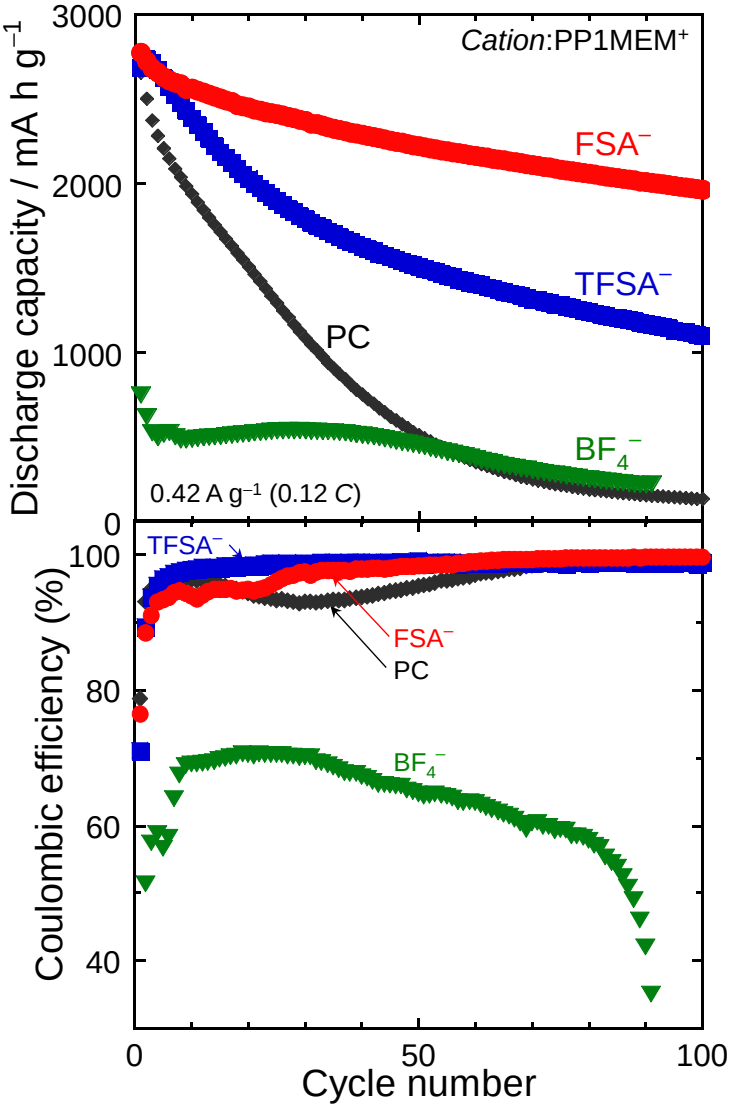

Figure 1 Dependence of (a) discharge capacity and (b) coulombic efficiency on cycle number for a Si electrode in 1 mol dm^{-3} Li*X*/PP1MEM-*X*. (*X*: FSA, TFSA, or BF_4) For comparison, the performance in 1 mol dm^{-3} LiTFSA/PC is also shown.

electrolytes. Figure S2 shows the first charge-discharge profiles of a Si electrode in various electrolytes. A potential plateau was observed at around 0.1 V vs. Li^+/Li during the charge (Li-insertion) process in all electrolytes, which corresponds to the Li–Si alloying reaction [4,5]. A huge irreversible capacity was confirmed at around 0.2 V vs. Li^+/Li on the charge curve in only the BF_4^--based electrolyte; an unfavorable reaction appears to occur on the Si electrode. The maximum Coulombic efficiency of the Si electrode in the BF_4^--based electrolyte was 70%, which was much lower than that in the other electrolytes, as shown in Figure 1(b). Generally, an ideal surface film formed on a negative electrode has very low electronic conductivity and high Li^+ conductivity, which suppresses continuous electrolyte decomposition. Therefore, the Coulombic efficiency increases after formation of the surface film. However, the Si electrode maintained low efficiency in the BF_4^--based electrolyte. This result suggests that the BF_4^--derived surface film did not function suitably as a protective film to prevent continuous electrolyte decomposition.

On the other hand, in the FSA^-- and $TFSA^-$-based electrolytes, the Si negative electrode exhibited a high initial discharge capacity of 2700 mA h g^{-1}, which is almost the same as that in the PC-based electrolyte. This result indicates that desolvation of Li^+ from anions occurred more readily in the FSA^-- and $TFSA^-$-based electrolytes than in the BF_4^--based electrolyte. To confirm this assumption, cyclic voltammetry for a simple redox reaction of Li was performed using a Ni electrode as a working electrode, as shown in Figure 2. A Ni working electrode was used because it does not change during the Li oxidation/reduction process. In all of the ionic liquid electrolytes, peaks

assigned to the deposition and dissolution of Li were observed at around –0.2 V and 0.1 V vs. Li^+/Li, respectively [21–23]. These peaks were large in the order FSA^-- > $TFSA^-$- > BF_4^--based electrolytes, which corresponds to the ionic association tendency of the Li salt [24]. This result indicates that the desolvation of Li^+ from the anion most easily occurs in the FSA^--based electrolyte, whereas the

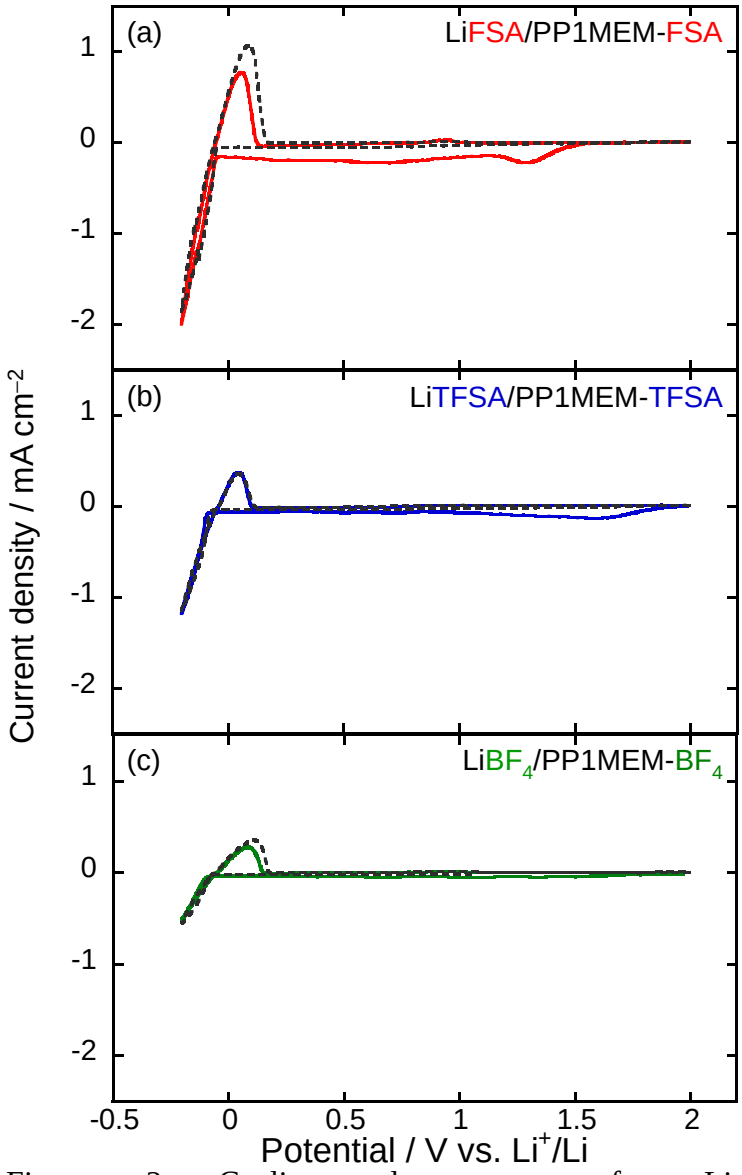

Figure 2 Cyclic voltammogram for Li deposition/dissolution on/from a Ni electrode in 1 mol dm^{-3} Li*X*/PP1MEM-*X*. (*X*: (a) FSA, (b) TFSA and (c) BF_4) Solid and dotted lines show first and second cycles, respectively. Scan rate : 1 mV s^{-1}

desolvation from BF_4^- does not occur as easily because of the stronger electrostatic interaction between Li^+ and BF_4^-. Therefore, the above assumption should be valid. In the first cycle, broad reduction peaks were observed at ca. 1.4 V and 1.6 V vs. Li^+/Li in the FSA^-- and $TFSA^-$-/ BF_4^--based electrolytes, respectively. Although the structure of the cation in all of the ionic liquids was the same, they had different reduction potentials. This suggests that the anion species in the electrolytes decomposed at each potential [25], and the surface film that consisted of the decomposition products should affect the cycling performance of the Si electrode.

The initial Coulombic efficiency in the FSA^-- and $TFSA^-$-based electrolytes was about 70% at the initial cycle and increased to almost 100% in the subsequent cycle. On the other hand, in the BF_4^--based electrolyte, the efficiency was lower in all cycles. This indicates that the surface films formed in the FSA^-- and $TFSA^-$-based electrolytes have much better insulation properties. Therefore, the FSA^-- and $TFSA^-$-derived surface films would act as a protective film to effectively prevent continuous decomposition of the electrolytes.

As shown in Figure 1(a), the electrode retained a discharge capacity of 2000 mA h g^{-1} after 100 cycles in the FSA^--based electrolyte, which is twice that in the $TFSA^-$-based electrolyte. It is considered that cycling stability is attributed to the difference of composition of the surface film. The surface film on Li electrode is composed of LiF, Li_2O, Li_2SO_4, $Li_2S_2O_4$, $Li_2NSO_2CF_3$, $Li_yC_2F_x$, $LiSO_2CF_3$ and others in TFSA-based electrolyte [26, 27]. On the other hand, the FSA-derived surface film is composed of LiF, LiOH, Li_2O, Li_2SO_4, SO_2F etc. [28, 29]. These insoluble Li salts on the

surface of the electrodes are probably responsible for the passivation of the electrodes. However, it is unclear that which component contributes to improve the cycling stability. Piper et al. investigated the decomposition mechanism of the FSA^- and $TFSA^-$ anions based on molecular dynamics simulations [29]. They reported that the S-F bond in FSA^- is broken preferentially, and F^- is rapidly released to form LiF, whereas LiF is not formed as readily in $TFSA^-$. It is well known that LiF improves the structural stability of the surface film [30]. Hence, the FSA^--derived surface film is more stable and should contribute to better cycling performance.

Although the FSA^--based ionic liquid electrolyte improved the cycling performance of the Si

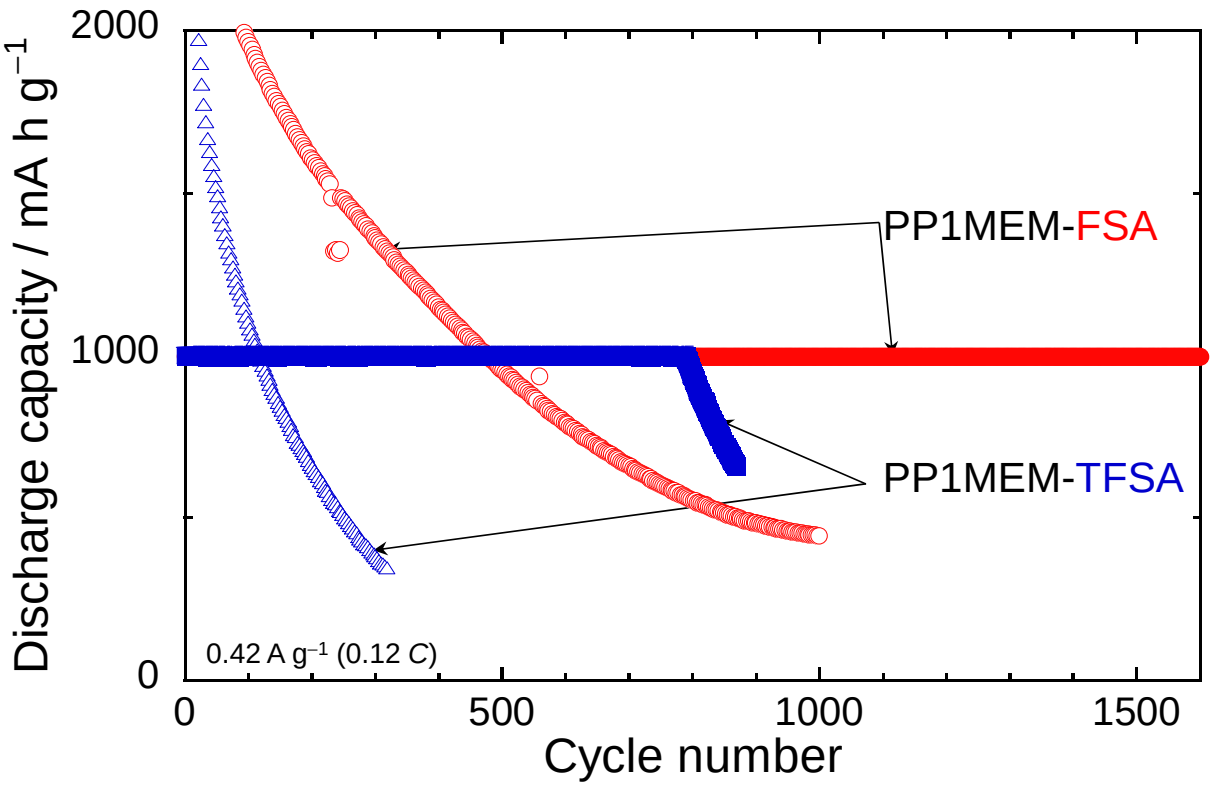

Figure 3 Variation in discharge capacity of a Si electrode in 1 mol dm^{-3} LiFSA/PP1MEM-FSA or LiTFSA/PP1MEM-TFSA versus number of cycles at a fixed Li-extraction level of 1000 mA h g^{-1}. For comparison, the performance without capacity limitation is also plotted.

electrode, gradual capacity-fading still occurred. We have demonstrated that the cycle performancecan be remarkably enhanced by controlling Li-insertion/extraction, in moderation [10].A charge-discharge cycling was performed with a Li-extraction capacity limitation of 1000 mA h g^{-1} in the FSA^-- and $TFSA^-$-based electrolytes, as shown in Figure 3. In the $TFSA^-$-based electrolyte, the Si electrode maintained a reversible capacity of 1000 mA h g^{-1} until about the 800th cycle. On the other hand, the Si electrode in the FSA^--based electrolyte exhibited better cycle performance with a discharge capacity of 1000 mA h g^{-1} even after ca. 1600 cycles. Capacity limitation dramatically improved the cycling stability, since the accumulation of severe stress was suppressed by moderation of the change in the volume of Si. Notably, the cycle life of the electrode in the FSA^--based electrolyte was twice as long as that in the $TFSA^-$-based electrolyte. Hence, the superiority of the FSA^--based electrolyte became clear when the capacity was limited.

Rate performance is one of the most important characteristics of LIBs, especially when used in an electric vehicle. Thus, the rate capability of a Si electrode in the ionic liquid electrolytes was investigated, as shown in Figure 4. The electrodes showed reversible capacities of 700 mA h g^{-1}, 100 mA h g^{-1}, and 1000 mA h g^{-1} at a high current rate of 6 *C* (21 A g^{-1}) in the FSA^--, $TFSA^-$-, and PC-based electrolytes, respectively. As shown in Table 1, the PC-based electrolyte exhibited the highest ionic conductivity of 5.51 mS cm^{-1}. In addition, the conductivity of the FSA^--based electrolyte (2.06 mS cm^{-1}) was three times that of the $TFSA^-$-based electrolyte (0.66 mS cm^{-1}). Since there are no electroneutral molecules in an ionic liquid, electrostatic interaction between the cation

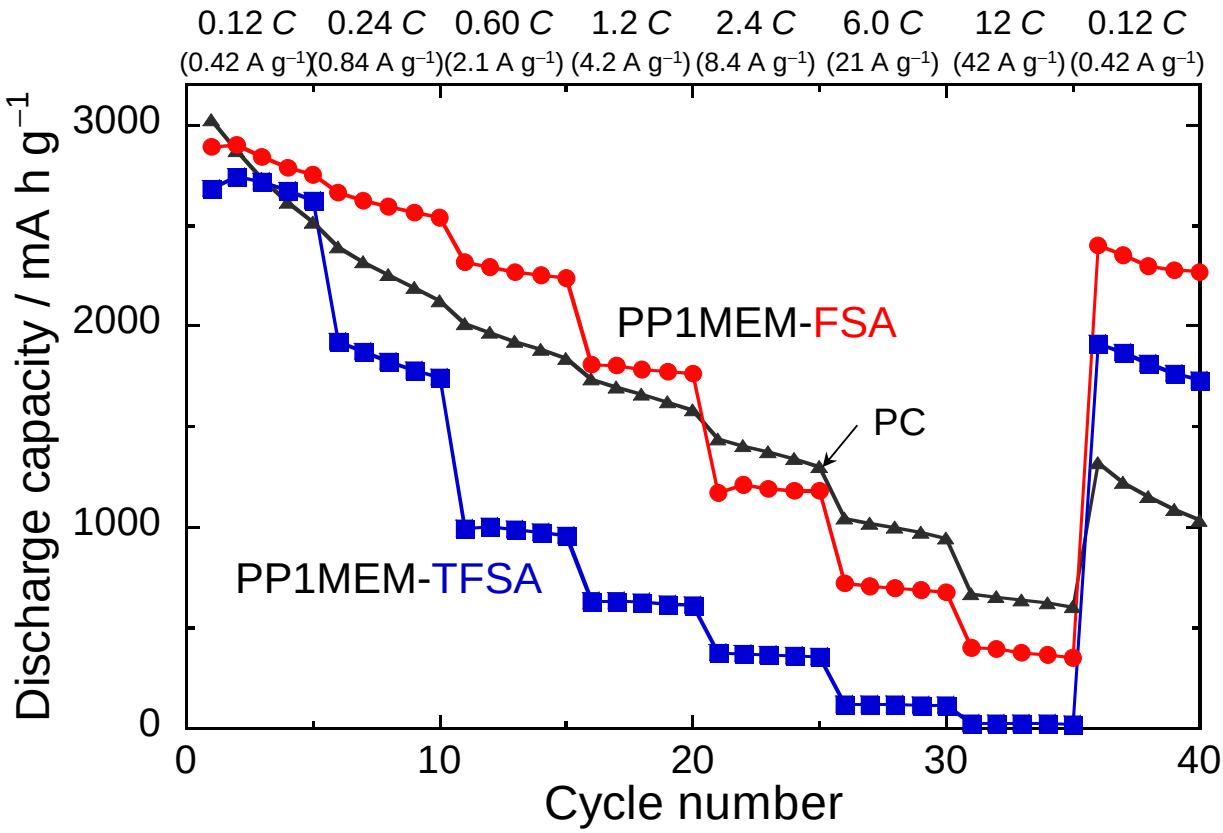

Figure 4. Rate capability for a Si electrode in 1 mol dm^{-3} LiFSA/PP1MEM-FSA, LiTFSA/PP1MEM-TFSA, and LiTFSA/PC at various current rates from 0.12 *C* to 12 *C*.

and anion immensely influences on the viscosity and ionic conductivity of the ionic liquid. The electrostatic interaction between Li^+ and FSA^- is weaker compared with it between Li^+ and $TFSA^-$. In addition, it has been confirmed that FSA-based ionic liquid shows a lower viscosity than TFSA-based one [31]. This is one of the reasons why FSA-based electrolyte has higher ionic conductivity compared to TFSA-based electrolyte.

Table 1 Ionic conductivity of electrolytes used in this study at 303 K.

Electrolyte		Conductivity / mS cm^{-1}
Li-salt	Solvent	
LiFSA	PP1MEM-FSA	2.06
LiTFSA	PP1MEM-TFSA	0.66
LiTFSA	PC	5.51

Li-insertion into a Si negative electrode proceeds via several steps: (1) Li^+ transport in the electrolyte bulk, (2) desolvation of Li^+ from ionic liquid anions or organic molecules, (3) Li^+ transport in an electric double layer and/or a solid electrolyte interphase, and (4) an alloying reaction of Si with Li [32].anions or organic molecules, (3) Li^+ transport in an electric double layer and/or a solid electrolyte interphase, and (4) an alloying reaction of Si with Li [32]. Under a high rate of 6 *C*, Li^+ transport, i.e. ionic conductivity in the electrolyte bulk, dominantly affects the rate capability. Consequently, a good high-rate performance was achieved only in the FSA^--based electrolyte, even though FSA^- and $TFSA^-$ are based on the same amide. When the current rate was back to the initial value of 0.12 *C*, the Si electrode showed a reversible capacity of 1200 mA h g^{-1} at the 36th cycle in the PC-based electrolyte. In contrast, the discharge capacity of the electrode recovered to 2500 and 2000 mA h g^{-1} at the 36th cycle in the FSA^-- and $TFSA^-$-based electrolytes, respectively, which are both higher than the capacity in the PC-based electrolyte. These results indicate that the Si electrode was disintegrated in the PC-based electrolyte at a high current rate of 6 *C*, whereas deterioration of the electrode was almost negligible in the FSA^-- and $TFSA^-$-based electrolytes. In addition, it is considered that the discharge capacity-fading in the FSA^-- and $TFSA^-$-based electrolytes at 6 *C* is mainly caused by limitation of the rate of Li^+ diffusion in the electrolyte bulk.

4. Conclusions

The effect of the structure of the anion in an ionic liquid electrolyte on the electrochemical

performance of a Si-alone negative electrode for use in LIBs was investigated. The electrode showed better cycle performance in FSA^-- and $TFSA^-$-based electrolytes than in a BF_4^--based electrolyte; the performance of the Si electrode is improved in some, but not all, ionic liquid electrolytes. The electric conductivities of the surface films formed in the FSA^-- and $TFSA^-$-based electrolytes would be lower than those in BF_4^-- and PC-based electrolytes. A Si-alone negative electrode also exhibited excellent cycle performance with a discharge capacity of 1000 mA h g^{-1} beyond 1600 cycles in the FSA^--based electrolyte under Li-extraction capacity limitation, which results from the structural stability of the surface film with LiF. A high rate performance was achieved with a reversible capacity of 700 mA h g^{-1} even at 6 *C* in the FSA^--based electrolyte due to the high conductivity of the electrolyte. Consequently, the FSA^--based ionic liquid electrolyte is the most promising electrolyte solution for next-generation LIBs with a Si-based negative electrode.

Acknowledgement

This work was partially supported by the Japan Society for the Promotion of Science (JSPS) KAKENHI, Grant-in-Aid for Scientific Research B (Grant 24350094) and Grant-in-Aid for Young Scientists B (Grant 15K21166).

References

[1] S.C. Lai, *J. Electrochem. Soc.* **123** (1976) 1196.

[2] M. N. Obrovac, L. Christensen, *Electrochem. Solid-State Lett.* **7** (2004) A93.

[3] T. D. Hatchard, J. R. Dahn, *J. Electrochem. Soc.* **151** (2004) A838.

[4] M. N. Obrovac, L. J. Krause, *J. Electrochem. Soc.* **154** (2007) A103.

[5] M. K. Datta, P. N. Kumta, *J. Power Sources* **194** (2009) 1043.

[6] T. Zhang, J. Gao, L. J. Fu, L. C. Yang, Y. P. Wu and H. Q. Wu, *J. Mater. Chem.* **17** (2007) 1321.

[7] T. Zhang, L. J. Fu, H. Takeuchi, J. Suzuki, K. Sekine, T. Takamura, Y. P. Wu, *J. Power Sources* **159** (2006) 349.

[8] H. Usui, Y. Yamamoto, K. Yoshiyama, T. Itoh, H. Sakaguchi, *J. Power Sources* **196** (2011) 3911.

[9] H. Usui, T. Masuda, H. Sakaguchi, *Chem. Lett.* **41** (2012) 521.

[10] M. Shimizu, H. Usui, T. Suzumura, H. Sakaguchi, *J. Phys. Chem. C* **119** (2015) 2975.

[11] M. Shimizu, H. Usui, K. Matsumoto, T. Nokami, T. Itoh, H. Sakaguchi, *J. Electrochem. Soc.* **161** (2014) A1765.

[12] K. Hayamizu, S. Tsuzuki, S. Seki, *J. Chem. Eng. Data* **59** (2014) 1944.

[13] K. Hayamizu, S. Tsuzuki, S. Seki, K. Fujii, M. Suenaga, Y. Umebayashi, *J. Chem. Phys.* **133** (2010) 194505.

[14] H. Matsumoto, H. Sakaebe, K. Tatsumi, *ECS Trans*. **16** (2009) 59.

[15] Y. Umebayashi, T. Mitsugi, S. Fukuda, T. Fujimori, K. Fujii, R. Kanzaki, M. Takeuchi, S. Ishiguro, *J. Phys. Chem. B* **111** (2007) 13028.

[16] Y. Umebayashi, S. Mori, K. Fujii, S. Tsuzuki, S. Seki, K. Hayamizu, S. Ishiguro, *J. Phys. Chem. B* **114** (2010) 6513.

[17] K. Fujii, H. Hamano, H. Doi, X. Song, S. Tsuzuki, K. Hayamizu, S. Seki, Y. Kameda, K. Dokko, M. Watanabe, Y. Umebayashi, *J. Phys. Chem. C* **117** (2013) 19314.

[18] T. Sugimoto, Y. Atsumi, M. Kikuta, E. Ishiko, M. Kono, M. Ishikawa, *J. Power Sources* **189** (2009) 802.

[19] T. Sugimoto, M. Kikuta, E. Ishiko, M. Kono, M. Ishikawa, *J. Power Sources* **183** (2008) 436.

[20] M. Yamagata, N. Nishigaki, S. Nishishita, Y. Matsui, T. Sugimoto, M. Kikuta, T. Higashizaki, M. Kono, M. Ishikawa, *Electrochim. Acta* **110** (2013) 181.

[21] C. Liu, X. Ma, F. Xu, L. Zheng, H. Zhang, W. Feng, X. Huang, M. Armand, J. Nie, H. Chen, Z. Zhou, *Electrochim. Acta* **149** (2014) 370.

[22] S. Fang, L. Yang, J. Wang, H. Zhang, K. Tachibana, K. Kamijima, *J. Power Sources* **191** (2009) 619.

[23] H. Matsumoto, H. Sakaebe, K. Tatsumi, M. Kikuta, E. Ishiko, M. Kono, *J. Power Sources* **160** (2006) 1308.

[24] P. Johansson, *Phys. Chem. Chem. Phys.* **9** (2007) 1493.

[25] P. C. Howlett, E. I. Izgorodina, M. Forsyth, D. R. MacFarlane, *Z. Phys. Chem.* **220** (2006) 1483.

[26] E. Markevich, R. Sharabi, V. Borgel, H. Gottlieb, G. Salitra, D. Aurbach, G. Semrau, M. A. Schmidt, *Electrochim. Acta* **55** (2010) 2687.

[27] S. Xiong, K. Xie, E. Blomberg, P. Jacobsson, A. Matic, *J. Power Sources* **252** (2014) 150.

[28] A. Budi, A. Basile, G. Opletal, A. F. Hollenkamp, A. S. Best, R. J. Rees, A. I. Bhatt, A. P. O'Mullane, S. P. Russo, *J. Phys. Chem. C* **116** (2012) 19789.

[29] D. M. Piper, T. Evans, K. Leung, T. Watkins, J. Olson, S. C. Kim, S. S. Han, V. Bhat, K. H. Oh, D. A. Buttry, S.-H. Lee, *Nat. Commun.* **6** (2015) 6230.

[30] K. Schroder, J. Alvarado, T. A. Yersak, J. Li, N. Dudney, L. J. Webb, Y. S. Meng, K. J. Stevenson, *Chem. Mater.* **27** (2015) 5531.

[31] S. Tsuzuki, K. Hayamizu, S. Seki, *J. Phys. Chem. B* **114** (2010) 16329.

[32] Y. Yamada, Y. Iriyama, T. Abe, Z. Ogumi, *J. Electrochem. Soc.* **157** (2010) A26.

Figure captions

Figure 1 Dependence of (a) discharge capacity and (b) Coulombic efficiency on cycle number for a Si electrode in 1 mol dm^{-3} Li*X*/PP1MEM-*X*. (*X*: FSA, TFSA, or BF_4) For comparison, the performance in 1 mol dm^{-3} LiTFSA/PC is also shown.

Figure 2 Cyclic voltammogram for Li deposition/dissolution on/from a Ni electrode in 1 mol dm^{-3} Li*X*/PP1MEM-*X*. (*X*: (a) FSA, (b) TFSA and (c) BF_4) Solid and dotted lines show the first and second cycles, respectively. Scan rate : 1 mV s^{-1}

Figure 3 Variation in discharge capacity of a Si electrode in 1 mol dm^{-3} LiFSA/PP1MEM-FSA or LiTFSA/PP1MEM-TFSA versus number of cycles at a fixed Li-extraction level of 1000 mA h g^{-1}. For comparison, performance without capacity limitation is also plotted.

Figure 4 Rate capability for a Si electrode in 1 mol dm^{-3} LiFSA/PP1MEM-FSA, LiTFSA/PP1MEM-TFSA, and LiTFSA/PC at various current rates from 0.12 *C* to 12 *C*.

Table 1 Ionic conductivity of electrolytes used in this study at 303 K.